Report No. KS-16-11 ▪ FINAL REPORT▪ October 2016

Long-Term Monitoring of a Pretensioned Concrete Bridge Near Winfield, Kansas

Robert J. Peterman, Ph.D., P.E.
Joseph R. Holste, Ph.D.

Kansas State University Transportation Center

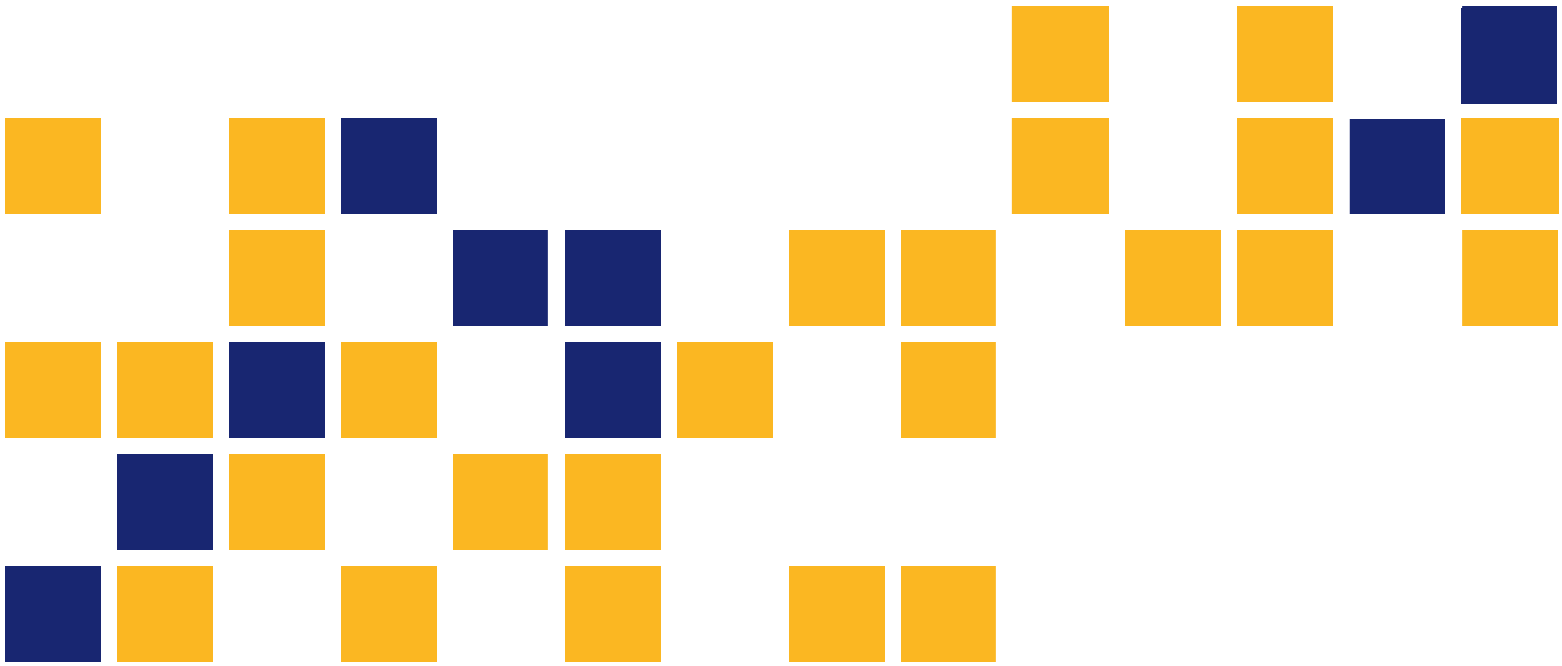

Kansas
Department of Transportation

1 Report No. KS-16-11	**2 Government Accession No.**	**3 Recipient Catalog No.**
4 Title and Subtitle Long-Term Monitoring of a Pretensioned Concrete Bridge Near Winfield, Kansas		**5 Report Date** October 2016 **6 Performing Organization Code**
7 Author(s) Robert J. Peterman, Ph.D., P.E., Joseph R. Holste, Ph.D.		**7 Performing Organization Report No.**
9 Performing Organization Name and Address Kansas State University Transportation Center Department of Civil Engineering 2113 Fiedler Hall Manhattan, KS 66506-5000		**10 Work Unit No. (TRAIS)** **11 Contract or Grant No.** C1887
12 Sponsoring Agency Name and Address Kansas Department of Transportation Bureau of Research 2300 SW Van Buren Topeka, Kansas 66611-1195		**13 Type of Report and Period Covered** Final Report December 2010–August 2016 **14 Sponsoring Agency Code** RE-0565-01
15 Supplementary Notes For more information write to address in block 9.		

The following report is an expansion of previous work conducted at Kansas State University and published as FHWA-KS-07-1 in April 2007 (Larson, Peterman, & Esmaeily, 2007). It details the findings from the long-term monitoring of a five-span bridge that was constructed in 2005 on US Highway 160 in Cowley County just west of Winfield, KS. The bridge utilized Type K3 pretensioned concrete girders that were fabricated by Prestressed Concrete, Inc., in Newton, KS. The girders in three of the spans were manufactured with conventional concrete while the girders in the remaining two spans were manufactured with self-consolidating concrete.

Seven of the girders used in the bridge were monitored to determine the time-dependent losses. This was done by using vibrating-wire strain gages that were embedded into the girders at the time of fabrication. Four of these instrumented girders contained conventional concrete, while three utilized self-consolidating concrete.

The results show that, after 8 years of installation, the self-consolidating concrete girders had higher long-term prestress losses than the conventional concrete girders. However, the average long-term losses for each mixture were still less than the predicted amounts. A visual inspection revealed no obvious differences in the performance of these girders, such as possible cracking, crazing, increased camber or deflection, or discoloration. The monitoring system, which consisted of embedded vibrating-wire strain gages and a solar-powered data logger, proved to be an excellent option for determination of long-term losses in pretensioned concrete bridge girders.

A flexural analysis of a continuous line of girders along the bridge superstructure was then conducted to determine if it would be possible to detect any differences in the flexural response of the girders in spans containing self-consolidating concrete and those containing conventional concrete due to realistic truck loads that could be applied during a load test. This analysis found that the K3 girders and composite concrete deck used in this bridge have such a large stiffness (moment of inertia) that it would not be possible to produce meaningful strain differences in the vibrating-wire strain gages under foreseeable test loads. The load test was therefore deemed not to be warranted.

17 Key Words Pretensioned Concrete, Long-Term Monitoring, Conventional Concrete, Self-Consolidating Concrete		**18 Distribution Statement** No restrictions. This document is available to the public through the National Technical Information Service www.ntis.gov.	
19 Security Classification (of this report) Unclassified	**20 Security Classification (of this page)** Unclassified	**21 No. of pages** 47	**22 Price**

Form DOT F 1700.7 (8-72)

This page intentionally left blank.

Long-Term Monitoring of a Pretensioned Concrete Bridge Near Winfield, Kansas

Final Report

Prepared by

Robert J. Peterman, Ph.D., P.E.
Joseph R. Holste, Ph.D.

Kansas State University Transportation Center

A Report on Research Sponsored by

THE KANSAS DEPARTMENT OF TRANSPORTATION
TOPEKA, KANSAS

and

KANSAS STATE UNIVERSITY TRANSPORTATION CENTER
MANHATTAN, KANSAS

October 2016

NOTICE

The authors and the state of Kansas do not endorse products or manufacturers. Trade and manufacturers names appear herein solely because they are considered essential to the object of this report.

This information is available in alternative accessible formats. To obtain an alternative format, contact the Office of Public Affairs, Kansas Department of Transportation, 700 SW Harrison, 2nd Floor – West Wing, Topeka, Kansas 66603-3745 or phone (785) 296-3585 (Voice) (TDD).

DISCLAIMER

The contents of this report reflect the views of the authors who are responsible for the facts and accuracy of the data presented herein. The contents do not necessarily reflect the views or the policies of the state of Kansas. This report does not constitute a standard, specification or regulation.

Abstract

The following report is an expansion of previous work conducted at Kansas State University and published as FHWA-KS-07-1 in April 2007 (Larson, Peterman, & Esmaeily, 2007). It details the findings from the long-term monitoring of a five-span bridge that was constructed in 2005 on US Highway 160 in Cowley County just west of Winfield, KS. The bridge utilized Type K3 pretensioned concrete girders that were fabricated by Prestressed Concrete, Inc., in Newton, KS. The girders in three of the spans were manufactured with conventional concrete while the girders in the remaining two spans were manufactured with self-consolidating concrete.

Seven of the girders used in the bridge were monitored to determine the time-dependent losses. This was done by using vibrating-wire strain gages that were embedded into the girders at the time of fabrication. Four of these instrumented girders contained conventional concrete, while three utilized self-consolidating concrete.

The results show that, after 8 years of installation, the self-consolidating concrete girders had higher long-term prestress losses than the conventional concrete girders. However, the average long-term losses for each mixture were still less than the predicted amounts. A visual inspection revealed no obvious differences in the performance of these girders, such as possible cracking, crazing, increased camber or deflection, or discoloration. The monitoring system, which consisted of embedded vibrating-wire strain gages and a solar-powered data logger, proved to be an excellent option for determination of long-term losses in pretensioned concrete bridge girders.

A flexural analysis of a continuous line of girders along the bridge superstructure was then conducted to determine if it would be possible to detect any differences in the flexural response of the girders in spans containing self-consolidating concrete and those containing conventional concrete due to realistic truck loads that could be applied during a load test. This analysis found that the K3 girders and composite concrete deck used in this bridge have such a large stiffness (moment of inertia) that it would not be possible to produce meaningful strain differences in the vibrating-wire strain gages under foreseeable test loads. The load test was therefore deemed not to be warranted.

Table of Contents

List of Tables

List of Figures

This page intentionally left blank.

Chapter 1: Introduction

This report documents the continuation of previous research that was conducted at Kansas State University and published in April 2007 (Larson, Peterman, & Esmaeily, 2007). In 2005, a five-span bridge containing 35 prestressed concrete girders was instrumented in order to determine long-term performance, including losses due to creep and shrinkage. The bridge is located on US Highway 160 in Cowley County just west of Winfield, KS, and each of the five spans was 50 ft long.

In order to determine the time-dependent losses in the girders, Geokon Model VCE-4200 vibrating-wire strain gages (VWSGs) were embedded into seven of the girders: four with conventional concrete (CON) and three with self-consolidating concrete (SCC; Geokon, Inc., 2004). The gages that were installed at the bottom row of strand (Figure 1.1) were then used by Larson et al. (2007) to establish the level of the prestress force in the girders during the first year after fabrication. This approach was similar to the one used by Yang and Myers (2005) to determine prestressed concrete losses in bridge girders.

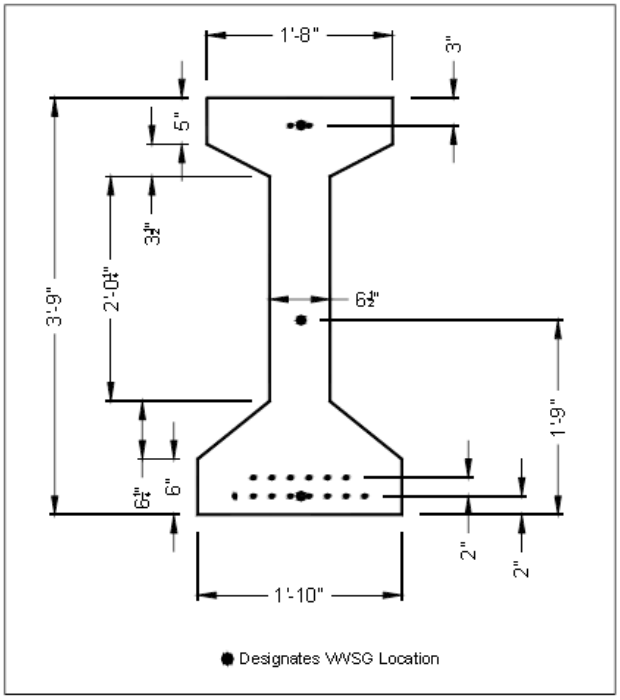

Figure 1.1: Location of Vibrating-Wire Strain Gages in Type K3 Girders
Source: Larson et al. (2007)

Of the 35 girders, 21 were cast with conventional concrete (Spans A, B, and C) and the remaining 14 girders with SCC (Spans D and E). The girders with embedded VWSGs were A3, B1, B3, C3, D1, D3, and E3 in Figure 1.2. The original project by Larson et al. (2007) monitored the bridge for 1 year after the girders were cast. Spans are ordered A through E from west to east.

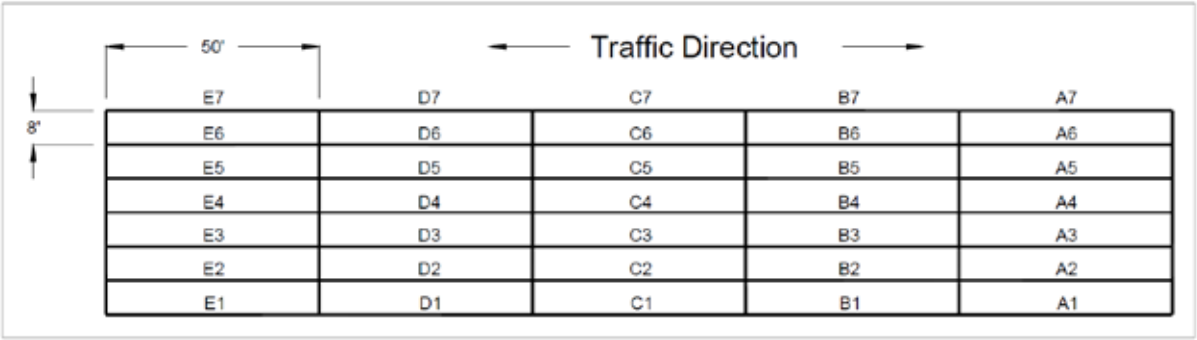

Figure 1.2: Girder Designation for Bridge
Source: Larson et al. (2007)

Since monitoring of the bridge was discontinued when the final report by Larson et al. (2007) was submitted to the Kansas Department of Transportation (KDOT), the primary goal of this project was to obtain new data from the instrumented girders in order to determine the losses that have occurred in the pretensioned concrete girders after being in service for more than 5 years.

Additionally, an analysis of the bridge was performed to determine if a load test could likely be used to detect any differences in the behavior of the bridge spans that were fabricated with girders utilizing the different concrete mixtures, CON and SCC.

Chapter 2: Current State of the Bridge and Instrumentation

This chapter provides information about the current state of the bridge and monitoring system. The bridge was visited twice as part of this project. On August 23, 2013, the monitoring system of the bridge was accessed. The data logger was still taking readings at this time. This indicated that the solar panel was working properly and still charging the battery. The data logger was removed from the bridge and taken to Kansas State University (KSU) for analysis.

Once at KSU, data from the data logger was initially unable to be downloaded since the original 8-year-old software was not compatible with current computers. Eventually, current software was obtained and the data logger was found to contain over 3 years of current data in its memory. These results are discussed in Chapter 3. The data logger had been previously programmed to collect data from each VWSG twice per day. The data logger has a "circular" buffer; therefore, only the most recent 3 years of data were able to be downloaded. All other data had been overwritten.

The second visit to the bridge occurred on May 14, 2014. During the visit, the main bridge elements were inspected visually, along with the various elements of the monitoring system.

Figure 2.1 shows the working solar panel attached to the side of the bridge. The battery level of the data logger indicated that the solar panel was charging the battery correctly. Figure 2.2 shows the main data logger that is attached to the girders along with the wires that connect to the VWSGs. The wires were not originally placed in any type of protective covering and were covered with bird droppings; however, all of the gages were still working so this apparently did not compromise the instrumentation.

The bridge was visually examined to determine any noticeable differences between the SCC and CON girders, such as possible cracking, crazing, increased camber or deflection, or discoloration. No visible differences were noted, and all girders appeared to be in excellent condition. Figures 2.3 and 2.4 show side views of the bridge and girders. Figure 2.5 shows the bottom of the girders and the deck. There was some efflorescence that was visible on the bottom side of the deck which is typical for many concrete bridge decks.

Figure 2.1: Solar Panel Mounted to Side of Bridge

Figure 2.2: Data Logger and Wires

Figure 2.3: Side View of Bridge

Figure 2.4: Close-Up View of Side of K3 Girders

Figure 2.5: Typical View of Girders and Deck Showing Effloresence

Chapter 3: Long-Term Vibrating-Wire Strain Gage Results

This chapter presents the results from the long-term monitoring of the five-span bridge. It provides comparisons between the girders that were manufactured with SCC and CON. It also provides the long-term prestress levels that were determined from the VWSGs.

Readings from the VWSGs that were stored in the data logger's memory were downloaded in 2013. The readings were analyzed along with the original readings obtained in 2005 and 2006 by Larson et al. (2007). The changes in strain indicated by the bottom VWSGs at mid-span were then used to calculate the reduction of stress in the prestressing strands due to long-term losses. This was done by multiplying the change in strain (since detensioning of the girders) by the modulus of elasticity (MOE) of the strands (assumed by Larson et al. to be 28,500 ksi). This change in stress of the strands was then subtracted from the initial prestress level (assumed by Larson et al. to be 202.5 ksi) to determine the effective prestress in the strands.

Figures 3.1 through 3.4 plot the effective prestress that was determined for the four CON girders, while Figures 3.5 through 3.7 plot the effective prestress that was determined for the three SCC girders. In these figures, the four CON girders are compared with the estimated long-term effective prestress value of 173 ksi calculated by Larson et al. (2007) using the Precast/Prestressed Concrete Institute (PCI, 2004) method for estimating prestress losses. The three SCC girders, however, are compared with the estimated long-term effective prestress value of 168 ksi. Larson et al. noted that the difference in these long-term prestress estimates was due primarily to higher initial loss of prestress from elastic shortening of the SCC girders.

As expected, in Figures 3.1 through 3.7, there is an overall trend of the effective prestress reducing with time. However, there are also consistent cycles or "bumps" in the data that have a period of approximately 365 days. These are likely due to thermal movements of the overall structure and represent about a 2 ksi seasonal change in the effective prestress.

In Figures 3.1 through 3.7, there are two cases where the indicated effective prestress was less than the values calculated by Larson et al. (2007). The first case was for Girder C3 (Figure 3.4). The long-term prestress indicated from the VWSG reading was approximately 159 ksi compared to the predicted value of 173 ksi.

The second case was for Girder E3 (Figure 3.7). For this girder, the long-term prestress indicated by the VWSG reading was approximately 156 ksi compared to the predicted value of 168 ksi. For Girder E3, the majority of the indicated loss occurred suddenly between the readings on Days 323 and 324 (refer to Figure 3.7).

It is hard to envision a realistic scenario where this could happen, since long-term losses are primarily due to creep and shrinkage of the concrete and there was no visible damage noted for this girder during the on-site bridge visit. Therefore, it is the opinion of the researchers that the sudden jump indicated around Day 324 is likely due to an anomaly in the instrumentation rather than due to a change in the structure itself. Accordingly, this jump has been removed from the data and the adjusted graph for Girder E3 is plotted in Figure 3.8. The long-term effective prestress value for Girder E3 that is listed in Table 3.1 is based on the adjusted graph (Figure 3.8).

This same instrumentation issue may have occurred for Girder C3, but the majority of the strain change happened during the time period when there is no available data, and hence there is no way to tell if the indicated strain change happened suddenly (as with Girder E3) or more gradually over time. As noted previously, the data logger did contain over 3 years of current data, collected at an interval of two scans per day. Still, approximately 3 years of data were overwritten due to the “circular” buffer of the data logger.

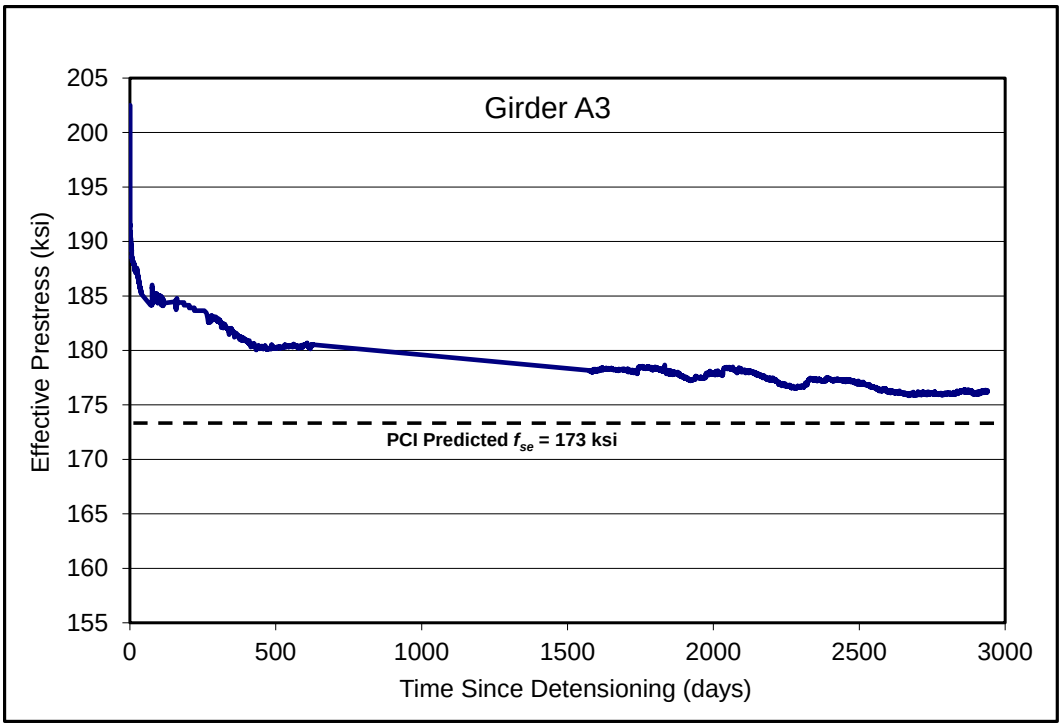

Figure 3.1: Effective Prestress Over Time for Girder A3

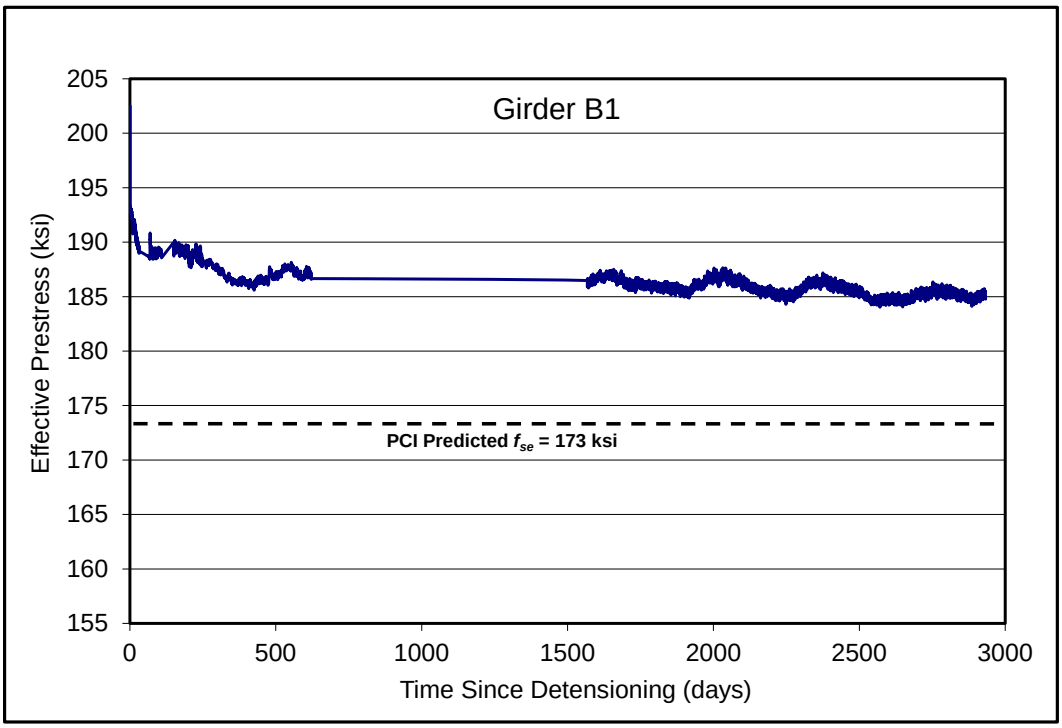

Figure 3.2: Effective Prestress Over Time for Girder B1

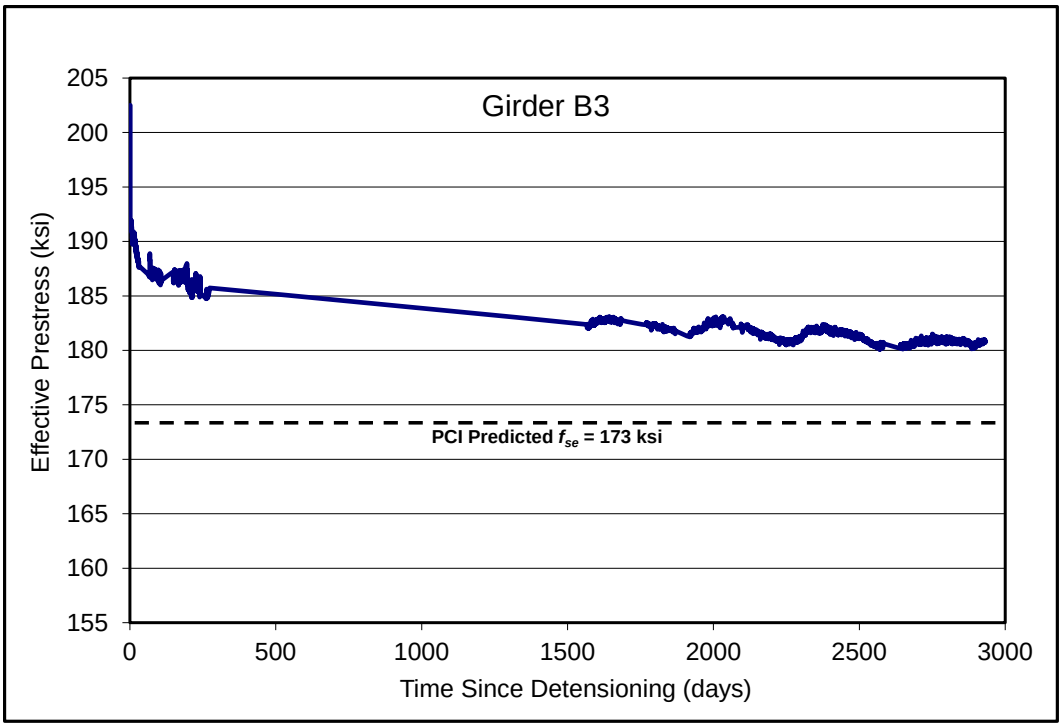

Figure 3.3: Effective Prestress Over Time for Girder B3

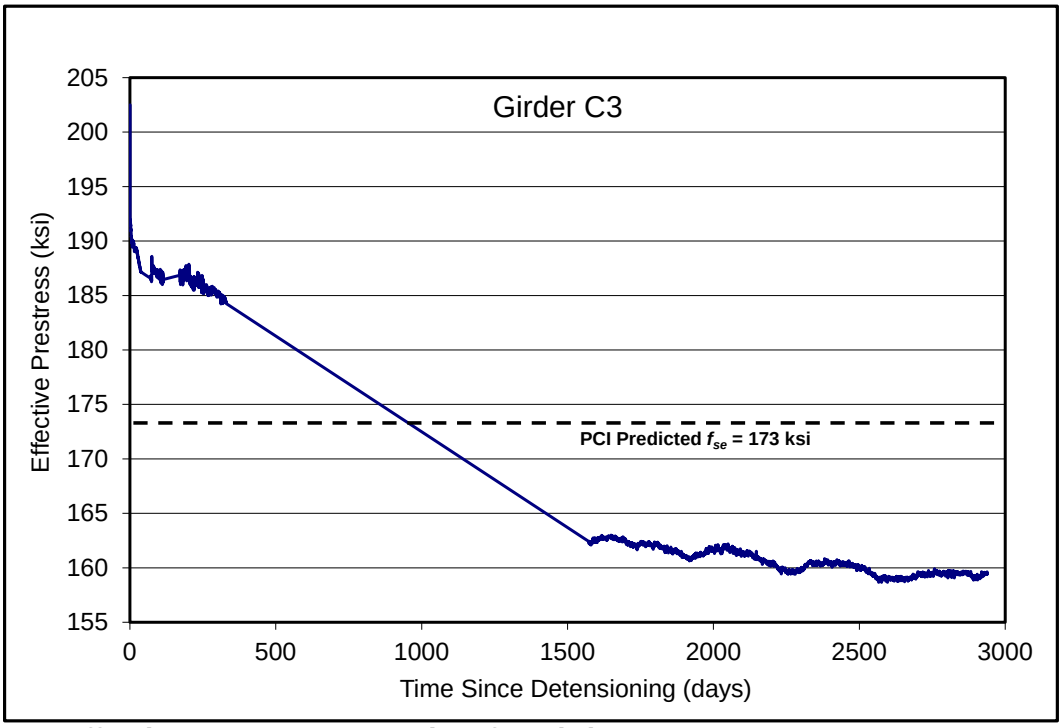

Figure 3.4: Effective Prestress Over Time for Girder C3

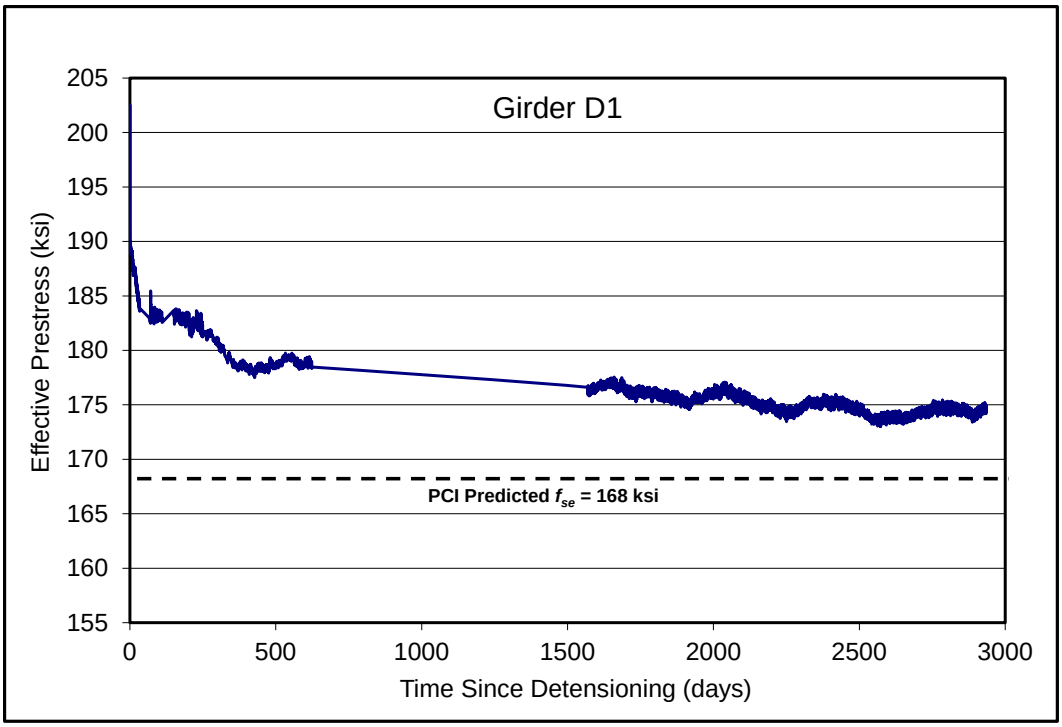

Figure 3.5: Effective Prestress Over Time for Girder D1

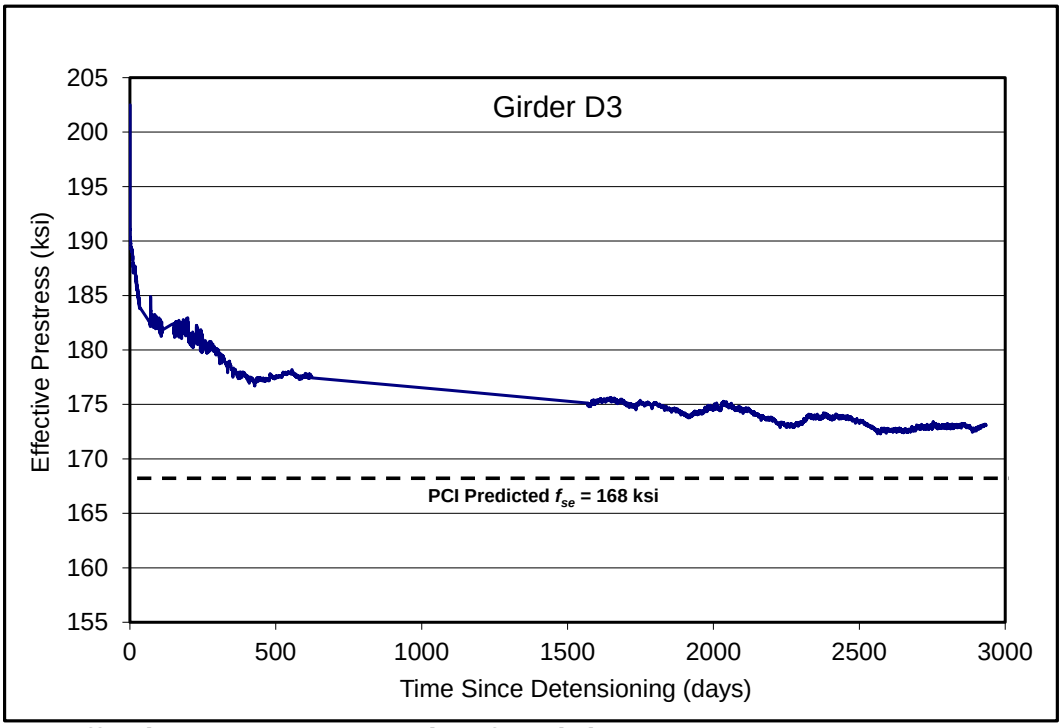

Figure 3.6: Effective Prestress Over Time for Girder D3

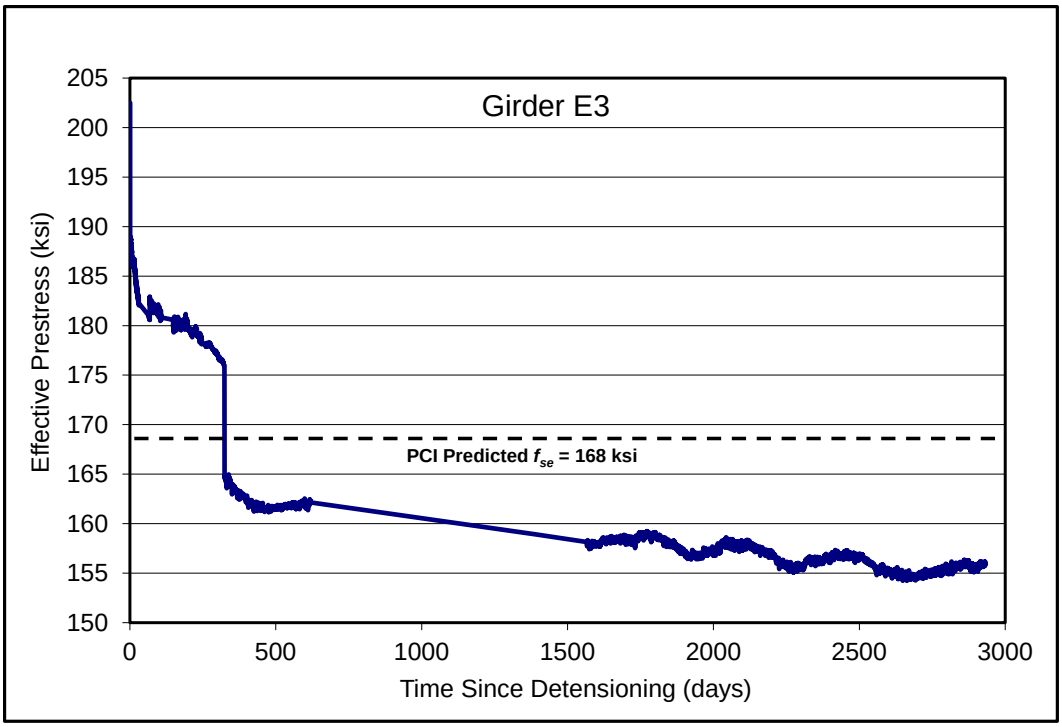

Figure 3.7: Effective Prestress Over Time for Girder E3

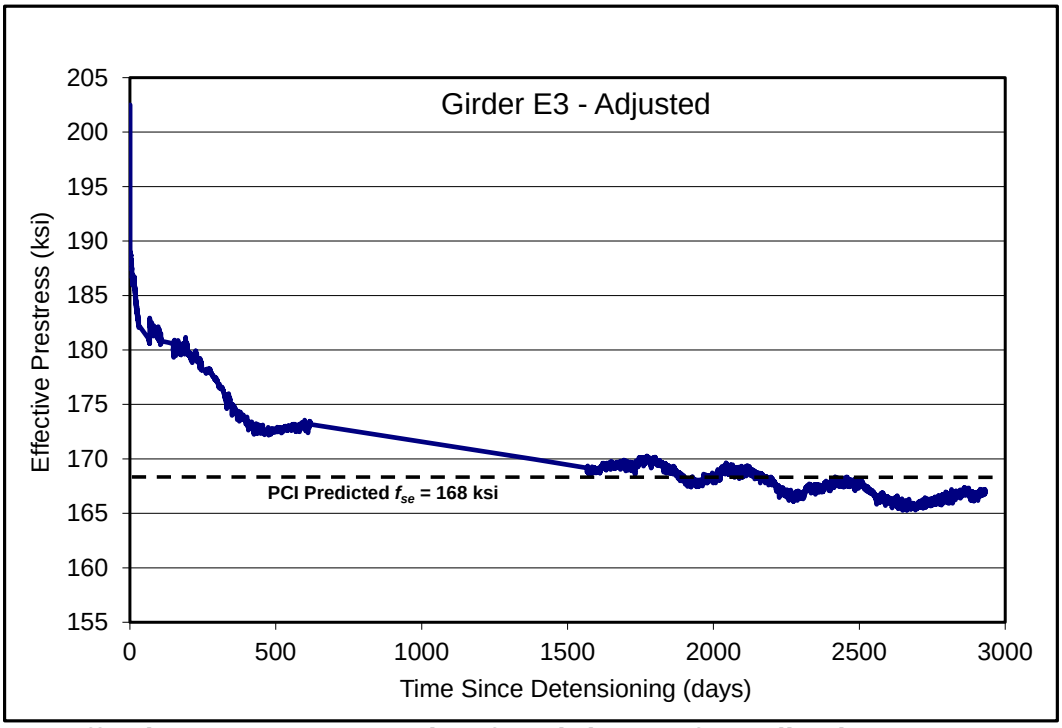

Figure 3.8: Effective Prestress Over Time for Girder E3 after Adjusting

The remaining (long-term) prestress for all girders is shown in Table 3.1. The average remaining prestress for all four CON girders was determined to be 175 ksi, which is slightly higher than the value of 173 ksi calculated by Larson et al. (2007). If Girder C3 is eliminated from the average, then the average long-term prestress in the CON girders would be 181 ksi. For the three SCC girders, the average remaining prestress is 171 ksi. This value is also slightly higher than the one predicted by Larson et al. of 168 ksi.

Table 3.1: Experimental versus Predicted Prestress

Girder		ACI/PCI Predicted Long-Term Prestress* (ksi)	Long-Term Prestress Indicated by VWSG Readings (ksi)	Average Long-Term Prestress Indicated by All VWSG Readings (ksi)	Average Long-Term Prestress After Eliminating Girder C3 (ksi)
CON	A3	173	177	175	181
	B1		185		
	B3		181		
	C3		159		
SCC	D1	168	174	171	171
	D3		173		
	E3		167		

*Source: Larson et al. (2007)

Figure 3.9 and Figure 3.10 compare the effective prestress over time for all of the CON and SCC girders, respectively. From Figure 3.9, it seems likely that the jump in the graph for Girder C3 may also be an anomaly. Figure 3.11 plots the effective prestress for all seven girders monitored, with the CON girders plotted in dark blue and the SCC girders in red. Figure 3.12 plots this same graph after eliminating Girder C3. From this graph, it is clear that the CON girders have a higher level of remaining prestress than the SCC girders, presumably due to the lower MOE of the SCC mixture as noted in Table 4.1 in Chapter 4.

Figure 3.13 provides still another way to view the data. In this graph, the girders in the end spans (Spans A and E) are colored light blue and pink, respectively. By comparing girders in the end and interior spans for each concrete type (compare dark blue lines with the light blue

line, and red lines with the pink line), the girders in the end span have a lower effective prestress than similar girders located in the first interior span.

The reason for this difference is unknown, but could possibly be due to differences of the end-restraint moments in the continuous bridge. Since higher prestress losses due to creep are typically caused by higher concrete compressive stresses at the level of the strands, this would suggest that the end-span girders may have lower sustained positive mid-span moments (higher compression) than the companion girders in the first interior span.

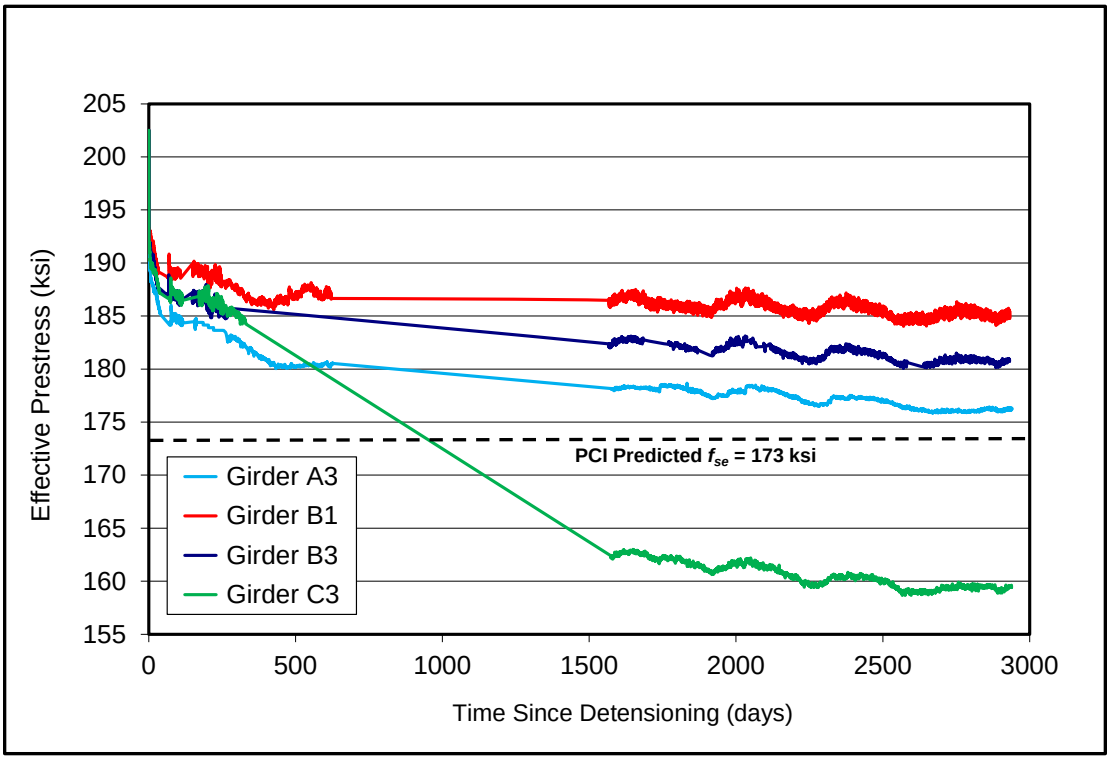

Figure 3.9: Comparison of Effective Prestress in CON Girders

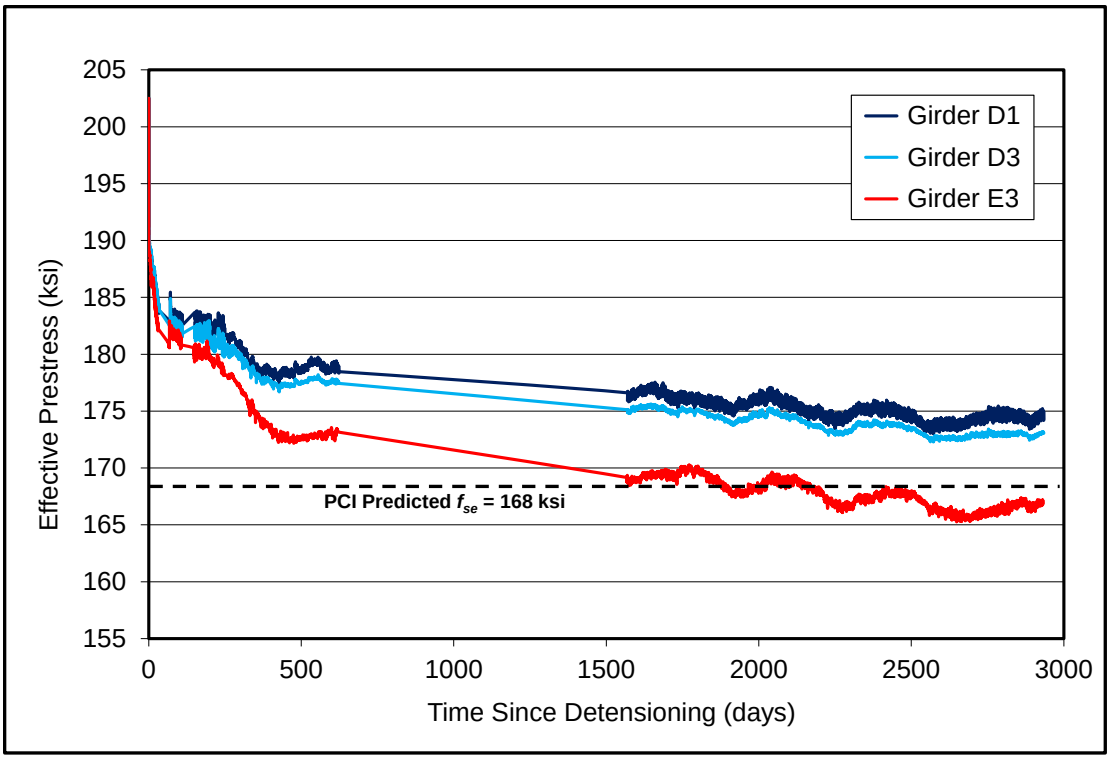

Figure 3.10: Comparison of Effective Prestress in SCC Girders

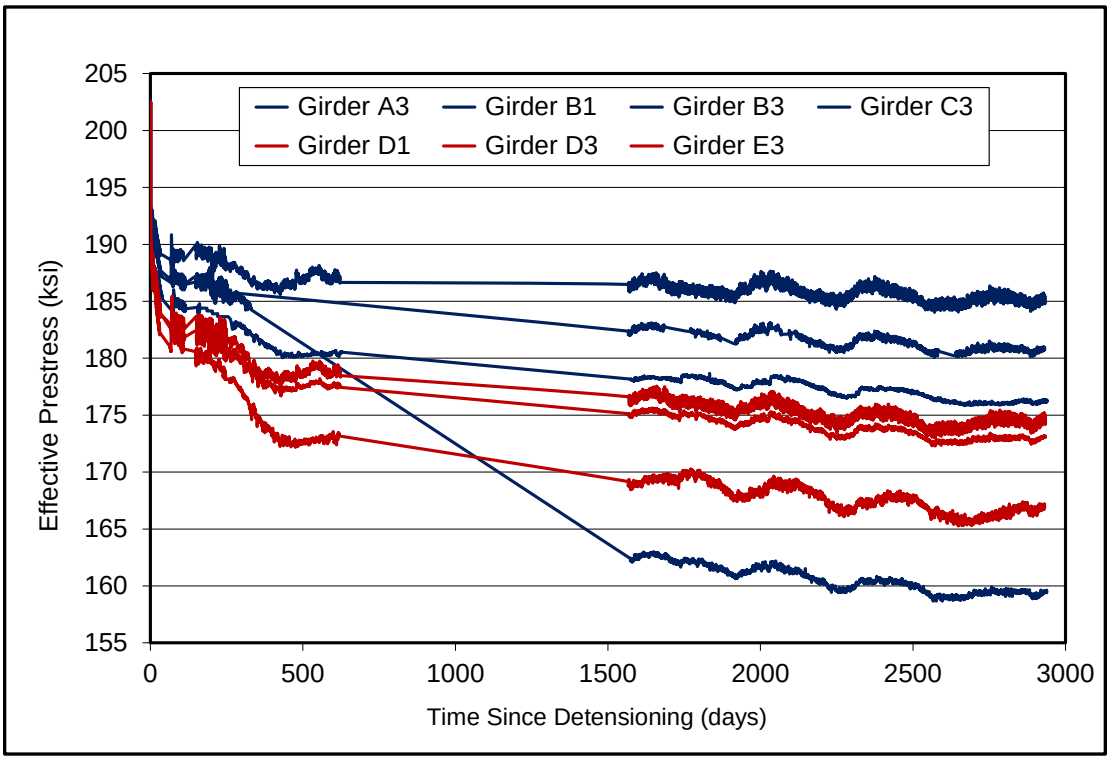

Figure 3.11: Comparison of Effective Prestress for All Seven Girders

Note: Blue = CON, Red = SCC

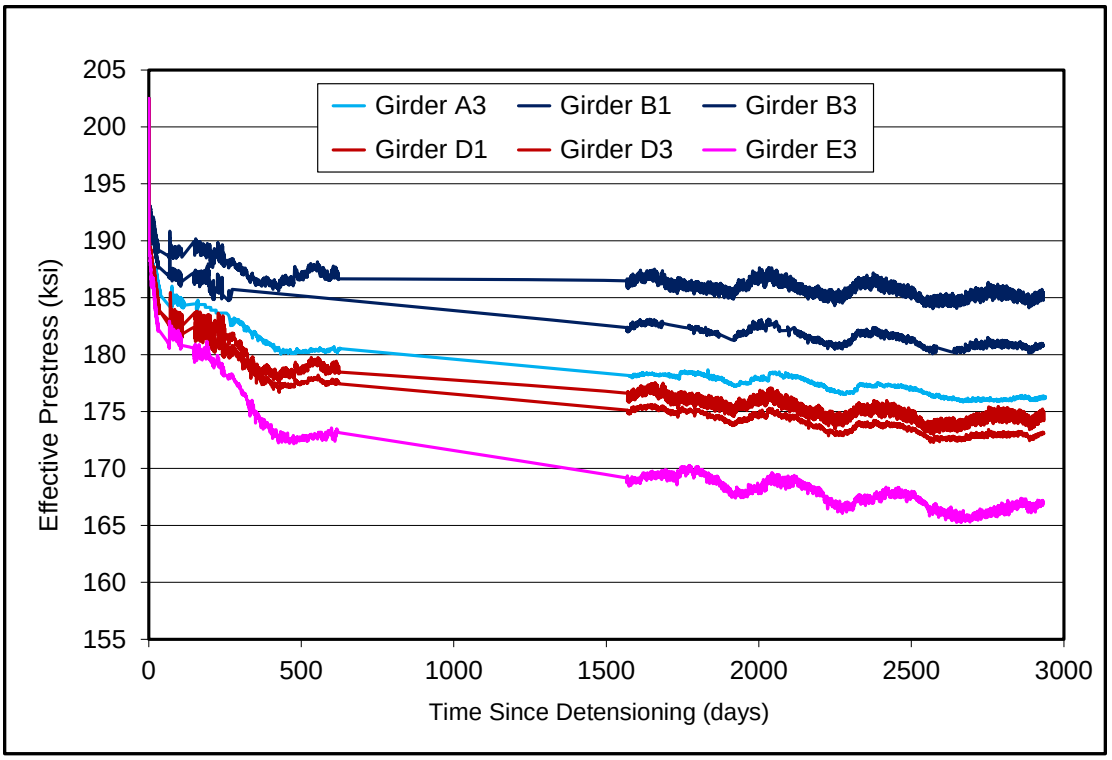

Figure 3.12: Comparison of Effective Prestress without Girder C3

Note: Blue = CON, Red = SCC

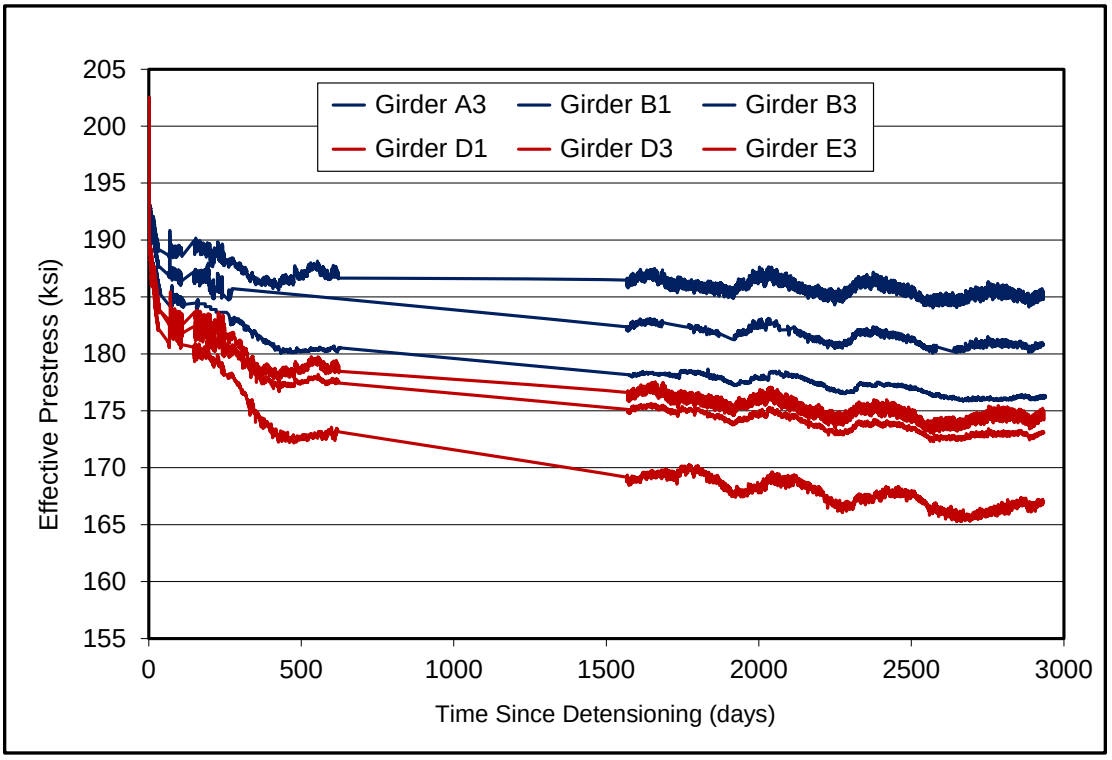

Figure 3.13: Comparison of Effective Prestress by Span

Note: Dark blue and red are the first interior span, while light blue and pink are end spans.

Chapter 4: Bridge Loading Analysis

This chapter details the theoretical results that would be expected from load testing the bridge. The predicted results were calculated to see if strain changes indicated by the VWSGs at mid-span of the girders during the loading process would be large enough to indicate a difference between the CON and SCC girders. If warranted by the analysis, the plan of the research team was to work with KDOT personnel to conduct a load test of the bridge using trucks filled with aggregate to try to detect any differences in the long-term performance of the spans manufactured with different concrete types.

The theoretical maximum moment for each girder was found by modeling a single line of girders along the bridge superstructure using RISA 2D (2001) software. Simple beam elements were used along with the transformed section properties of the girders. For the analysis, the end-supports were modeled as pinned connections, since this would result in the maximum possible mid-span moments and the analysis would thus be an upper-bound case. Larson et al. (2007) reported the properties of the K3 girders. The girders had an overall height of 45 inches, a cross-sectional area of 525 in^2, and a distance from the girder bottom to the centroid of the cross-section of 21 inches. The K3 girders had a nominal moment of inertia of 127,490 in^4.

The transformed section properties were calculated by transforming the area of the cast-in-place concrete deck into the properties of the K3 girder concrete. This is consistent with other analyses used to determine live-load distribution in bridge-girder systems (Ambare & Peterman, 2001; Barker & Puckett, 1997; Bishara, Liu, & El-Ali, 1993; Zokaie, Osterkamp, & Imbsen, 1991). In order to perform this calculation, the 28-day MOE values that were reported by Larson et al. (2007) were used. These are shown in Table 4.1.

Larson et al. (2007) reported that the 28-day MOE of the bridge deck concrete was higher than the 28-day MOE of both the CON and SCC girders. This may be due to different aggregate sources that were used for the deck and girder mixes. Larson et al. reported that limestone aggregates were used for the girder concrete. Unfortunately, these same researchers did not report the source or type of aggregates that were used in the bridge deck concrete.

Table 4.1: 28-Day Modulus of Elasticity

Member	Modulus of Elasticity
CON Girders	4600 ksi
SCC Girders	3750 ksi
Bridge Deck	5150 ksi

Source: Larson et al. (2007)

Transformed section properties used to model a single line of continuous girders are shown in Table 4.2. Since the deck concrete had a higher MOE than the bridge girders, deck widths larger than the center-to-center spacing of the girders are used to calculate the transformed composite section properties, since the deck concrete is transformed into girder concrete by the ratio (MOE_{deck}/MOE_{girder}). Actual deck widths used to calculate the transformed section properties are listed in Table 4.2. Spans 1, 2, and 3 were modeled with CON composite properties, while Spans 4 and 5 were modeled with SCC composite properties (Figure 4.1).

Alternatively, the analysis could be conducted by transforming the girder concrete into deck concrete. In this case, a deck width of 96 inches would be used and all girder-width dimensions would be reduced by the modular ratio of MOE_{girder}/MOE_{deck}.

Table 4.2: Transformed Composite Section Properties

Girder Type	Modulus of Elasticity (ksi)	Composite Deck Width (in.)	Composite Moment of Inertia ($in.^4$)	Y_{bot} (in.)
SCC	3750	131.8	419,096	40.24
CON	4600	107.5	398,686	38.95

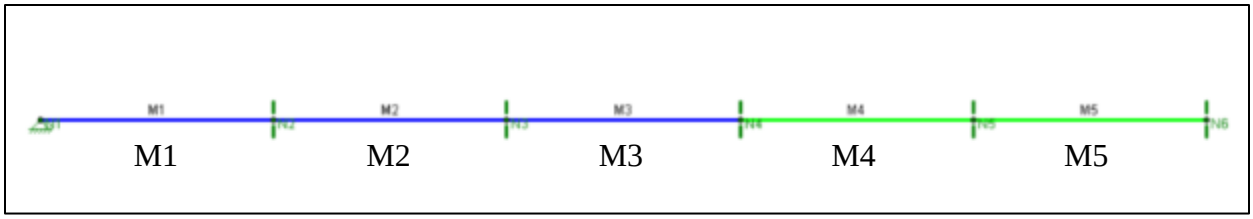

Figure 4.1: RISA 2D Setup of Five-Span Bridge

Note: Blue = CON, Green = SCC

4.1 One MD 3S2 Truck

The initial truck that was applied to the continuous girder line of the RISA 2D model was an MD 3S2 truck (Figure 4.2). This truck has some of the highest axle weights of the typical trucks used in bridge rating. The axle loads were moved across the bridge model at 1-ft intervals in both directions, and the complete moment envelope generated. Figure 4.3 shows the MD 3S2 moving load being applied to the bridge girder-line model and the resulting moment envelope shape that was obtained by analysis of the structure when the moving load was placed at all locations, with positive moments plotted below the axis. The peak positive mid-span moment values from Figure 4.3 are listed in Table 4.3.

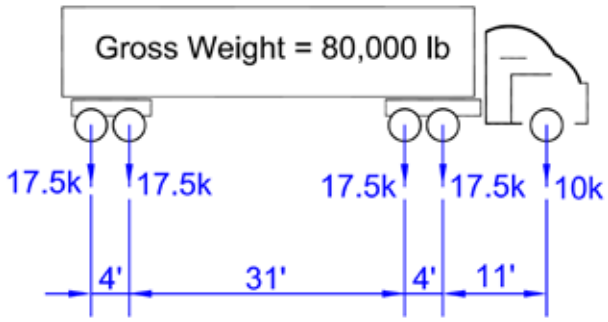

Figure 4.2: Load and Spacing of MD 3S2 Truck

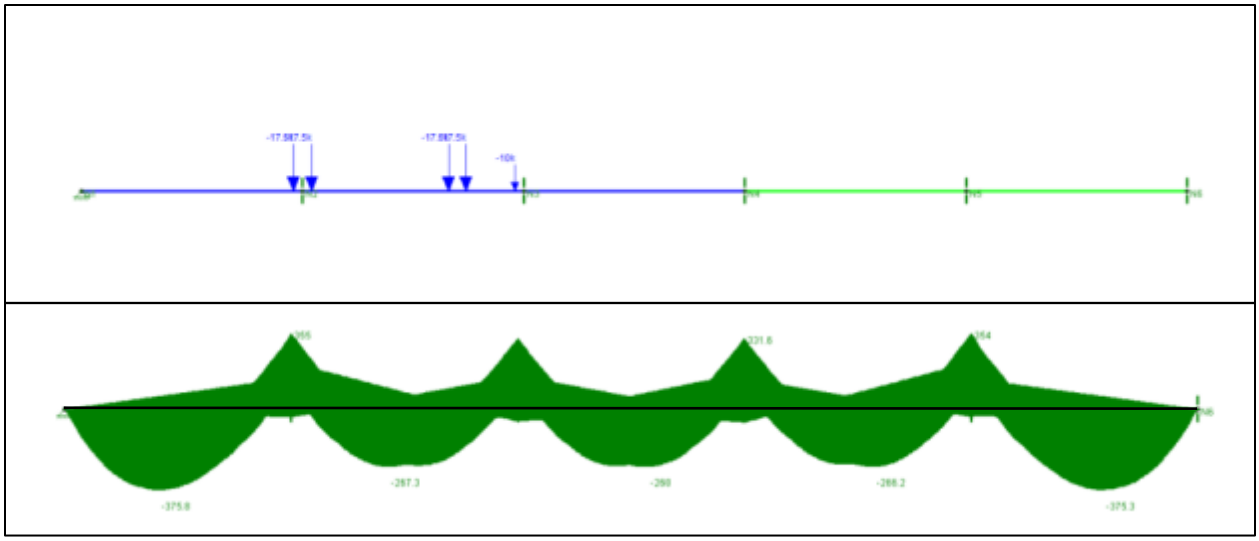

Figure 4.3: Moment Envelope of One MD 3S2 Truck Moving Load, RISA 2D

4.2 Two MD 3S2 Trucks

The next case was to investigate the situation where two of these trucks would be placed back-to-back as shown in Figure 4.4 and allowed to move across the bridge at 1-ft intervals. Figure 4.5 shows the back-to-back moving load being applied to the RISA 2D model and the resulting moment envelope. The peak positive mid-span moment values from Figure 4.5 are listed in Table 4.3.

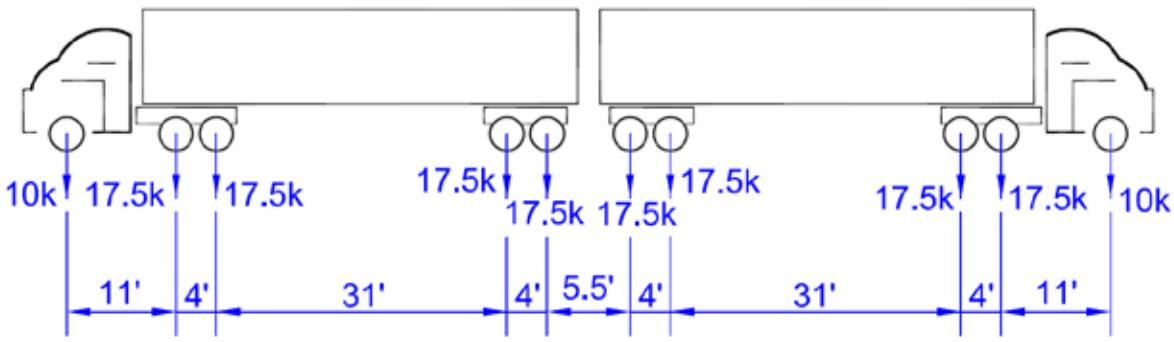

Figure 4.4: Axle Loads and Spacing of Two MD 3S2 Trucks Placed End to End

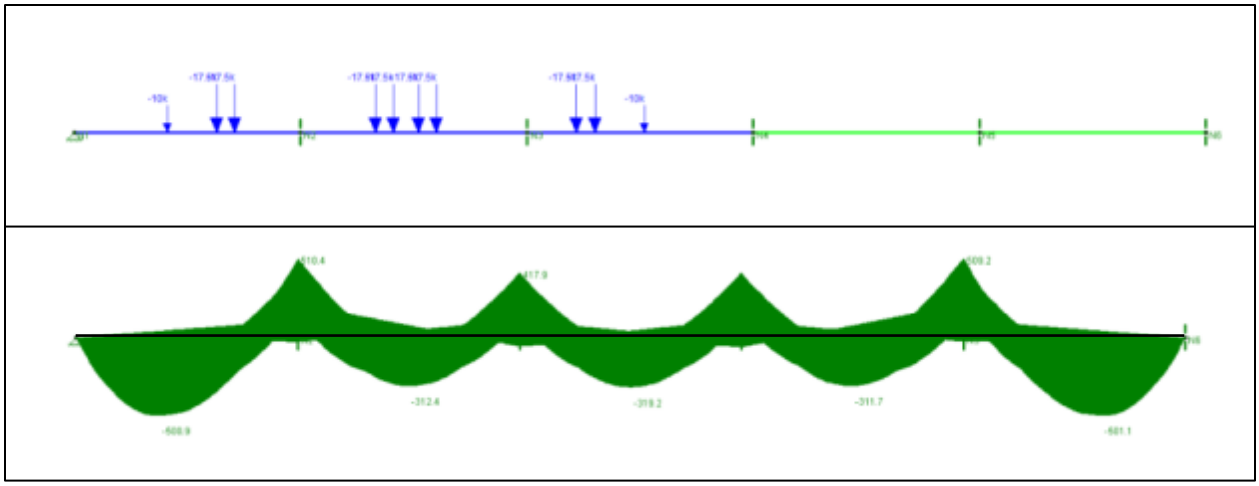

Figure 4.5: Moment Envelope, Two Back-to-Back MD 3S2 Trucks Moving Load, RISA 2D

Table 4.3: Maximum Mid-Span Positive Moments Due to MD 3S2 Moving Loads, kip-ft

Loading Case	CON			SCC	
	Span 1	Span 2	Span 3	Span 4	Span 5
One MD 3S2 Truck	375.8	267.3	268.0	266.2	375.3
Two MD 3S2 (Back-to-Back)	500.9	312.4	319.2	311.7	501.2

When viewing Table 4.3, the mid-span moments that need to be compared for each loading case are those for Spans 1 and 5, and Spans 2 and 4. (Note: Spans 1 to 3 have CON girders, and Spans 4 and 5 have SCC girders.) For example, if we consider the end span with CON girders, the maximum moment due to two back-to-back MD 3S2 trucks is 500.9 kip-ft, while the same moment for the end span with SCC girders is 501.2 kip-ft.

If all of the girders had been manufactured with the same concrete (either CON or SCC), then the theoretical moment envelope would be perfectly symmetrical. However, due to the different concrete types and the resulting different transformed section properties, there is a very slight asymmetric force distribution within the statically-indeterminate structure.

Also, since the MD 3S2 trucks have a 31-ft spacing between the closest front and rear axles (refer to Figure 4.2), when one set of axles is near the center of a 50-ft span (causing a positive mid-span moment), the other set of axles is in the adjacent span which acts to reduce the moment at the center of the span.

4.3 AASHTO Tandem Vehicle

Because the MD 3S2 trucks have a relatively large axle spacing, it was decided during a meeting with KDOT in March 2015 to also consider the American Association of State Highway and Transportation Officials' "Tandem" vehicle that consists of two 25-kip axle loads spaced 4 ft apart (refer to Figure 4.6; AASHTO, 2014).

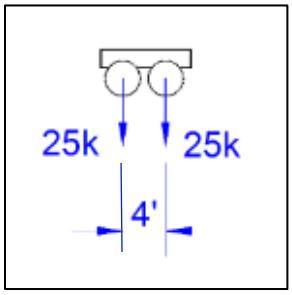

Figure 4.6: Axle Loads and Spacing for Tandem Vehicle

The position for placement of the tandem vehicles was determined by generating influence lines for the mid-span moments in both Span 1 and Span 2. The influence lines were constructed by positioning a 1-kip load every 5 ft ($1/10^{th}$ points) along the entire bridge and then determining the resulting mid-span moment (the location of the vibrating-wire gages) that is produced in Spans 1 and 2. These moments are then plotted as a function of the distance the point load is located from the end of the bridge. The influence line for the mid-span moment in Span 1 is shown in Figure 4.7, while the influence line for the mid-span moment in Span 2 is shown in Figure 4.8.

Please note that similar influence lines could also be drawn for Spans 4 and 5. These would be nearly identical in shape to the ones drawn for Spans 1 and 2 except they would be mirrored (symmetrically) about the center line of the bridge. The reason that they would be nearly identical is because the slight differences between transformed section properties of the CON and SCC girders do not result in much asymmetry in the internal force and moment distribution.

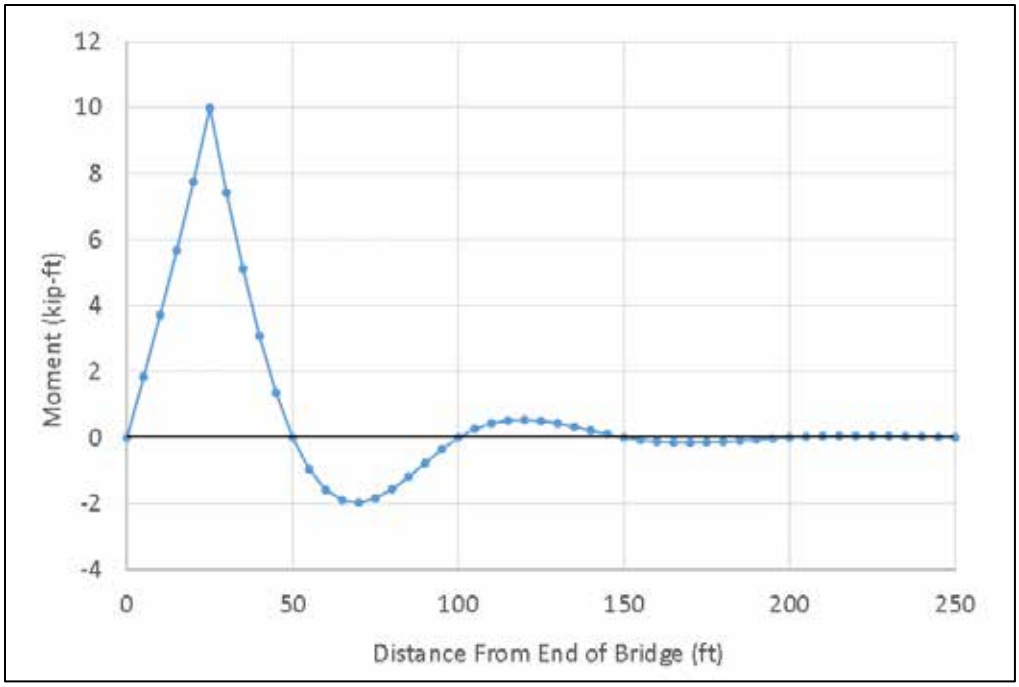

Figure 4.7: Influence Line for the Mid-Span Moment in Span 1

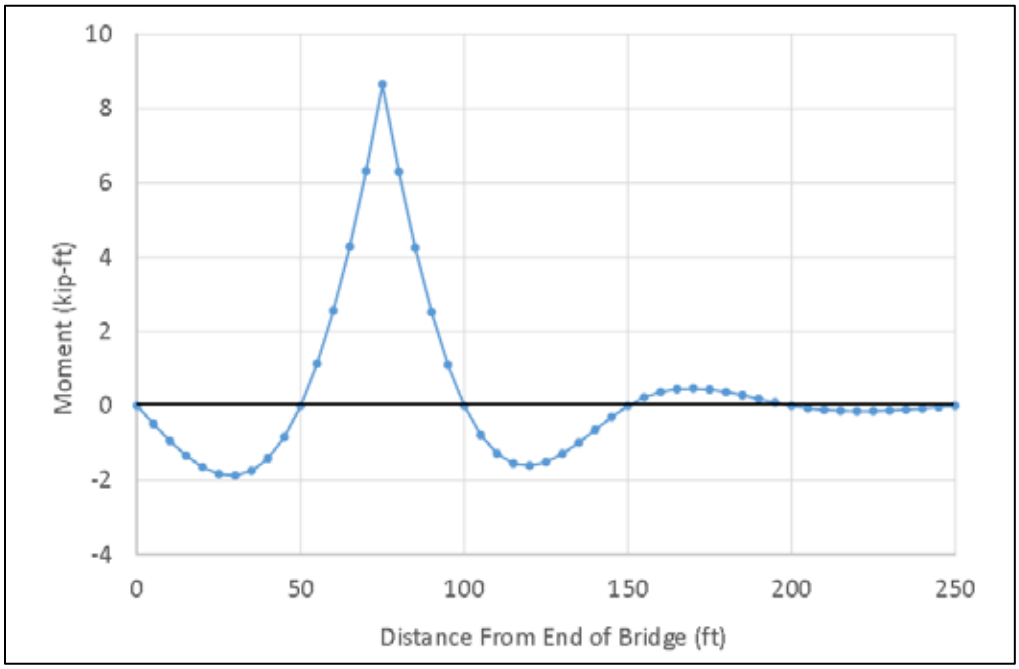

Figure 4.8: Influence Line for the Mid-Span Moment in Span 2

Thus, three additional cases were investigated with tandem vehicles strategically placed on the RISA 2D model. These included tandem trucks positioned in Spans 1 and 3 (Figure 4.9) to determine the maximum mid-span moment in Span 1; tandem trucks positioned in Spans 3 and 5 (Figure 4.10) to determine the maximum mid-span moments in Span 5; and tandem trucks positioned in Spans 2 and 4 (Figure 4.11) to determine the maximum mid-span moments in Spans 2 and 4.

Note from Figure 4.7 that the maximum mid-span moment in Span 1 would theoretically be higher if Span 5 were also loaded in addition to Spans 1 and 3. However, this difference is negligible and the actual structure has more fixity than the RISA 2D model with pinned end-supports, meaning that the additional moment would be even smaller than implied in Figure 4.7. The mid-span moments resulting from these three additional load scenarios are presented in Table 4.4.

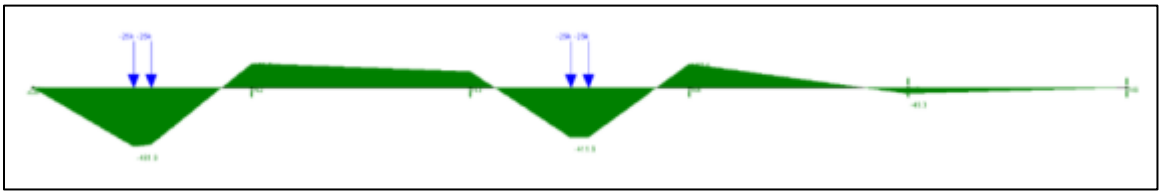

Figure 4.9: Span 1, Tandem Truck Placement, Maximum Mid-Span Moment and Moment Diagram

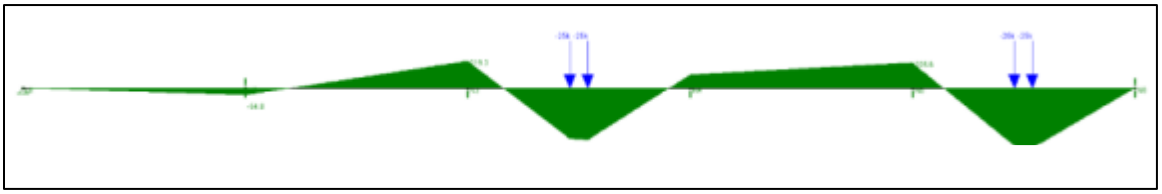

Figure 4.10: Span 5, Tandem Truck Placement, Maximum Mid-Span Moment Diagram

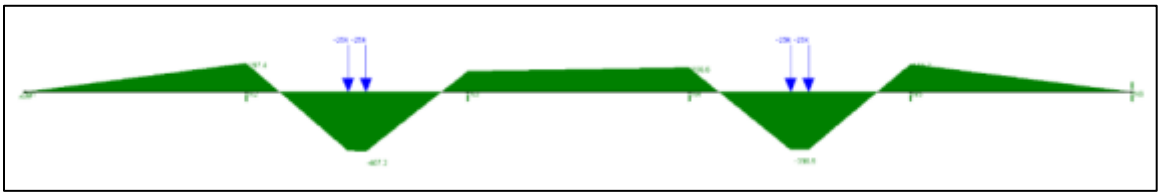

Figure 4.11: Spans 2 and 4, Tandem Truck Placement, Maximum Mid-Span Moment Diagram

Table 4.4: Tandem Vehicles, Mid-Span Maximum Positive Moments, kip-ft

Loading Case	CON			SCC	
	Span 1	Span 2	Span 3	Span 4	Span 5
Tandems in Spans 1 and 3	475.3	Negative	409.5	Negative	24.7
Tandems in Spans 3 and 5	27.4	Negative	410.9	Negative	472.2
Tandems in Spans 2 and 4	Negative	405.4	Negative	396.1	Negative

From Table 4.4, the maximum difference in CON and SCC girder-line mid-span moments due to AASHTO (2014) Tandem vehicles can be achieved by loading Spans 2 and 4. This difference is from 405.4 kip-ft for the CON girders to 396.1 kip-ft for the SCC girders.

4.4 Additional Single Truck Used in KDOT Load Rating

Per KDOT's direction, the researchers also performed an additional RISA 2D analysis with a single 22-ton gross weight truck that is currently used in bridge load rating (refer to Figure 4.12). KDOT Bridge Evaluation Engineer John Culbertson confirmed that only one truck of this type is placed on a bridge at a time as part of the bridge load rating process. Mr. Culbertson also said that he could not think of a case where more than one of these trucks would be placed on a bridge at one time (J. Culbertson, personal communication, July 12, 2016).

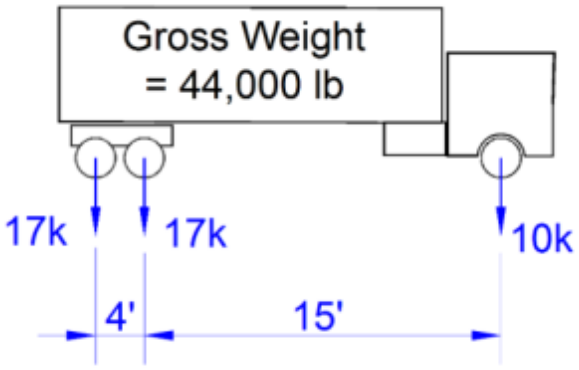

Figure 4.12: 22-Ton Truck Currently Used in Bridge Load Rating

Based on this phone conversation, the RISA 2D analysis was performed with one 22-ton truck that could travel in either direction. The axle loads were moved across the bridge model at 1-ft intervals in both directions, and the complete moment envelope was generated.

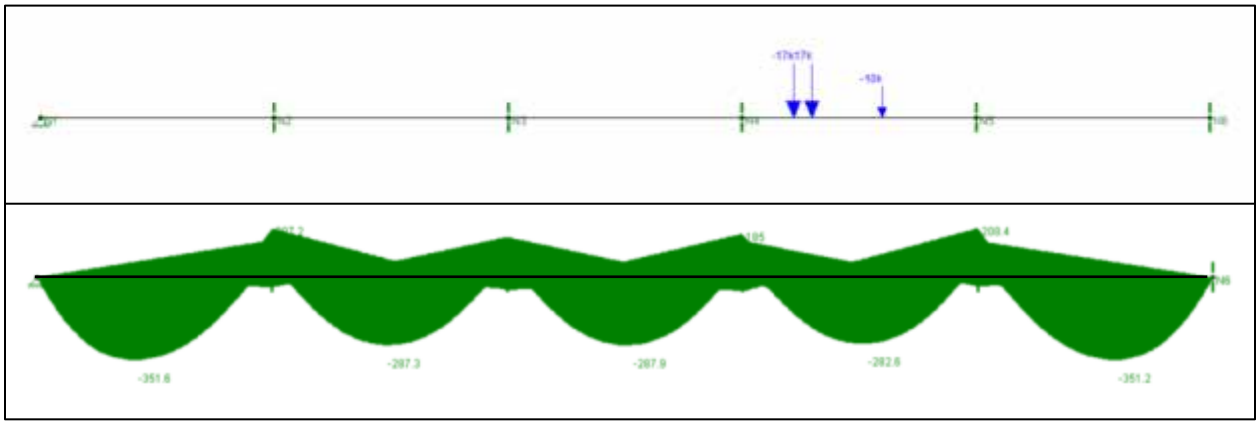

Figure 4.13: One 22-Ton Truck Moving Load Moment Envelope, RISA 2D

Figure 4.13 shows the 22-ton truck moving load being applied to the bridge girder-line model and the resulting moment envelope shape that was obtained by analysis of the structure when the moving load was placed at all locations, with positive moments plotted below the axis. The peak positive moment values from Figure 4.13 are listed in Table 4.5.

Table 4.5: Mid-Span Positive Moments Due to One 22-Ton Truck in kip-ft

Loading Case	CON			SCC	
	Span 1	Span 2	Span 3	Span 4	Span 5
One 22-Ton Truck	351.6	287.3	287.9	282.6	351.2

4.5 Summary of Results from Different Loading Cases

The maximum mid-span moments from the loading cases presented above are consolidated and reviewed in this section. Table 4.6 lists these moments for each span and loading condition. It is the intent of this analysis to make a direct comparison between the expected strain levels in spans where the pretensioned girders were manufactured using SCC and CON. Therefore, the spans that can be directly compared for the 5-span bridge are the end spans

(Spans 1 and 5) and the first interior spans (Spans 2 and 4). There is not a direct comparison for the center span (Span 3) which was cast with CON.

Table 4.6: Summary of Positive Mid-Span Moments from Various Loading Cases, kip-ft

Loading Case	CON			SCC	
	Span 1	Span 2	Span 3	Span 4	Span 5
One MD 3S2 Truck	375.8	267.3	268.0	266.2	375.3
Two MD 3S2 (Back-to-Back)	500.9	312.4	319.2	311.7	501.2
Tandems in Spans 1 and 3	475.3	Negative	409.5	Negative	24.7
Tandems in Spans 3 and 5	27.4	Negative	410.9	Negative	472.2
Tandems in Spans 2 and 4	Negative	405.4	Negative	396.1	Negative
One 22-Ton Truck	351.6	287.3	287.9	282.6	351.2

Table 4.7 shows the direct comparison of mid-span positive moments due to the different loading scenarios for the bridge end spans (Spans 1 and 5), while Table 4.8 shows a similar comparison for the first interior bridge spans (Spans 2 and 4).

Table 4.7: Comparison of Mid-Span Moments, Spans 1 and 5, Single Lane Loading, kip-ft

Loading Case	CON	SCC
	Span 1	Span 5
One MD 3S2 Truck	375.8	375.3
Two Back-to-Back MD 3S2 Trucks	500.9	501.2
Two Tandem Trucks	475.3	472.2
One 22-Ton Truck	351.6	351.2

Table 4.8: Comparison of Mid-Span Moments, Interior Spans 2 and 4, One Lane Loading, kip-ft

Loading Case	CON	SCC
	Span 2	Span 4
One MD 3S2 Truck	267.3	266.2
Two Back-to-Back MD 3S2 Trucks	312.4	311.7
Two Tandem Trucks	405.4	396.1
One 22-Ton Truck	287.3	282.6

When reviewing the mid-span moment data from Table 4.7 and Table 4.8, it is important to remember that these moments would not be carried entirely by a single girder line. However, since the distribution of moments is based on the relative stiffness of each span, using the transformed section properties of a single girder line is sufficient to accurately determine the distribution of moments between the adjacent spans.

Since the two-lane bridge is seven girders in width, the moments due to a single lane of traffic need to be divided by 3.5 girders. It is important to note that the bridge near Winfield, KS, is significantly wider than needed for the current two lanes of traffic, presumably so that it can accommodate up to four lanes of traffic in the future. Table 4.9 and Table 4.10 list the theoretical mid-span positive moments in a girder that were obtained by dividing the lane loading by 3.5 girders.

Table 4.9: Comparison of Mid-Span Moments in a Single Girder, Spans 1 and 5, kip-ft

Loading Case	CON	SCC
	Span 1	Span 5
One MD 3S2 Truck	107.4	107.2
Two Back-to-Back MD 3S2 Trucks	143.1	143.2
Two Tandem Trucks	135.8	134.9
One 22-Ton Truck	100.5	100.3

Table 4.10: Comparison of Mid-Span Moments in a Single Girder, Spans 2 and 4, kip-ft

Loading Case	CON	SCC
	Span 2	Span 4
One MD 3S2 Truck	76.4	76.1
Two Back-to-Back MD 3S2 Trucks	89.3	89.1
Two Tandem Trucks	115.8	113.2
One 22-Ton Truck	82.1	80.7

4.6 Calculation of Theoretical Mid-Span Elastic Strain Due to Static Loading

In order to calculate the theoretical mid-span strains that could be expected in the vibrating-wire gages due to the different loading cases, the moments in Table 4.9 and Table 4.10 are first used to calculate the theoretical stress at that location by:

$$\sigma = \frac{My}{I} \qquad \textbf{Equation 4.1}$$

Where:

M is the mid-span moment,

y is the distance from the neutral axis of the transformed section to the location of the vibrating-wire strain gage, and

I is the moment of inertia of the composite transformed section.

The effective width was determined to be 96 inches based on Section 8.10.1.1 of the AASHTO (2002) *Standard Specifications for Highway Bridges*. The effective width of the flange is the lesser of:

- ¼ of the effective span length,
- 12 times the slab thickness plus ½ the beam flange width, or
- Beam spacing.

The composite moment of inertia of the CON K3 girders with an 8.5-inch-thick deck and an effective width of 96 inches was calculated to be 398,686 in^4 and the location of the centroid (Y_{bot}) from the bottom of the beam was calculated at 38.95 inches (refer to Table 4.2). Therefore, since the lower-most vibrating-wire gage is located 2 inches from the bottom of the beam (Figure

1.1), the distance "y" at the location of the vibrating-wire gage is equal to 38.95 – 2 = 36.95 inches. Hence, the stress at the gage location may be determined as:

$$\sigma = \frac{M*y}{I} = \frac{M*(36.95\ in)}{398{,}686\ in^4}$$

From Table 4.10, the moment at the mid-span of Span 2 (CON) due to the Tandem truck loading was 115.8 kip-ft. Accordingly, the stress at the vibrating-wire gage location at the mid-span of Span 2 due to the Tandem truck loading would be:

$$\sigma = \frac{(115{,}800\ lb-ft)(\frac{12in}{ft})(36.95\ in)}{398{,}686\ in^4} = 129\ psi$$

Since the modulus of elasticity of the CON mix at 28 days was reported by Larson et al. (2007) to be 4600 ksi, the theoretical instantaneous strain change in the concrete is then calculated as:

$$\varepsilon = \frac{\sigma}{E} = \frac{129\ psi}{4{,}600{,}000\ psi} = 0000280 = 28.0 \text{ microstrain} \qquad \textbf{Equation 4.2}$$

Similarly, from Table 4.10, the moment at the mid-span of Span 4 (SCC) due to the Tandem truck loading was 113.2 kip-ft. The composite moment of inertia of an SCC K3 girder with an 8.5-inch-thick deck and an effective width of 96 inches was calculated to be 419,096 in^4 and the location of the centroid (Y_{bot}) from the bottom of the beam was calculated at 40.24 inches (refer to Table 4.2). Using a similar approach as above, the theoretical stress in the concrete at the level of the bottom VWSGs was determined to be 123.9 psi (where y = 40.24 – 2 = 38.24 in.). The modulus of elasticity of the SCC mix at 28 days was reported by Larson et al. (2007) to be 3750 ksi. Using Equation 4.2, the strain the concrete is calculated to be 33.0 microstrain.

This same procedure was used to estimate the theoretical elastic strain change at the mid-span vibrating-wire gage locations for each loading case. These values of strain are presented in Table 4.11 and Table 4.12. From these two tables, it is clear that the maximum difference in

theoretical elastic strain that could be expected between the vibrating-wire gages in the SCC and CON gages would be only 7.2 microstrain (the value shaded yellow in Table 4.11).

Table 4.11: Theoretical Mid-Span Elastic Strain Change in Spans 1 and 5, Microstrain

Loading Case	CON	SCC	Difference
	Span 1	Span 5	
One MD 3S2 Truck	26.0	31.3	5.3
Two Back-to-Back MD 3S2 Trucks	34.6	41.8	7.2
Two Tandem Trucks	32.8	39.4	6.6
One 22-Ton Truck	24.3	29.3	5.0

Table 4.12: Theoretical Mid-Span Elastic Strain Change in Spans 2 and 4, Microstrain

Loading Case	CON	SCC	Difference
	Span 2	Span 4	
One MD 3S2 Truck	18.5	22.2	3.7
Two Back-to-Back MD 3S2 Trucks	21.6	26.0	4.4
Two Tandem Trucks	28.0	33.0	5.0
One 22-Ton Truck	19.8	23.6	3.7

Note, if twice the number of trucks were employed over half of the bridge width during a load test (to take advantage of the fact that the bridge is wide enough to accommodate 4 lanes of traffic), then there would be twice the moment divided by 3.5 girder lines, which increases the maximum theoretical difference from 7.2 to 14.4 microstrain.

This low amount of theoretical strain difference would be impractical, if not impossible, to measure (with the current VWSG and data logging instrumentation) during a load test since other factors (including placement of vehicles, thermal drift, etc.) would produce strain readings that are much larger than the differences caused by the girder concrete modulus of elasticity. Therefore, a load test of the bridge is not warranted.

Chapter 5: Conclusions

Based on the findings presented herein, the following conclusions may be drawn.

1. The bridge was visually examined to determine any noticeable differences between the SCC and CON girders, such as possible cracking, crazing, increased camber or deflection, or discoloration. No visible differences were noted, and all girders appeared to be in excellent condition.
2. The data monitoring system, which consisted of vibrating-wire strain gages and a solar-powered data logger, was working properly after being installed for over 8 years. The longevity of this monitoring system shows that it is an excellent option for monitoring bridges for many years without maintenance. However, due to software and hardware technology constantly changing, it is recommended that the data should be downloaded at a minimum of every two years. This frequency may correspond well with routine bridge inspections.
3. The vibrating-wire gage strain readings indicate that, as predicted, the SCC girders had higher long-term losses than the CON girders after 8 years of service. However, both mixes resulted in average long-term effective prestress values that were still larger than those predicted by Larson et al. (2007) using standard prestress-loss equations.
4. Experimental load testing of the bridge was determined by analysis to not be warranted, since differences in the composite section properties of the CON and SCC girders are relatively small, and it is not possible to apply enough load over the relatively short spans to achieve any appreciable difference in behavior.

Chapter 6: Recommendations for Implementation

Since visual inspection showed that the SCC girders are performing similarly to the CON girders after 8 years of service, and since the average long-term effective prestress in the SCC girders was determined to be higher than predicted by Larson et al. (2007), there is no need for KDOT to limit the use of SCC in the fabrication of pretensioned concrete girders. Because of the potential benefits of using SCC, which include improved surface appearance and the reduced risk of honey-combing and improper consolidation, the authors recommend that KDOT make SCC the preferred mixture for pretensioned concrete bridge girders used on Kansas bridges.

This research also revealed that long-term losses in SCC girders can be reasonably estimated using the relatively simple PCI (2004) method.

In addition, because the vibrating-wire gages and solar-powered data logger were fully functional after 8 years of installation without servicing, this type of instrumentation may be utilized whenever KDOT has questions about long-term stresses or load paths in concrete structures. Based on the findings in this report, data collection could be done on either an annual or biennial basis depending on the buffer size, number of sensors, and frequency of readings.

References

Ambare, S., & Peterman, R. (2001). Rapid replacement of bridges using prestressed concrete inverted tees: Live-load distribution concerns. In C. Shield & A. Schultz (Eds.), *Proceedings of the Fifth National Workshop on Bridge Research in Progress, October 8-10, 2001, Minneapolis, Minnesota*. Minneapolis, MN: University of Minnesota.

American Association of State Highway and Transportation Officials (AASHTO). (2002). *Standard specifications for highway bridges* (17th ed). Washington, DC: Author.

American Association of State Highway and Transportation Officials (AASHTO). (2014). *AASHTO LRFD bridge design specifications, customary U.S. units* (7th ed.). Washington, DC: Author.

Barker, R.M., & Puckett, J.A. (1997). *Design of highway bridges*. New York, NY: Wiley-Interscience.

Bishara, A.G., Liu, M.C., & El-Ali, N.D. (1993). Wheel load distribution on simply supported skew I-beam composite bridges. *Journal of Structural Engineering*, *119*(2), 339–419.

Geokon, Inc. (2004). *Installation manual: Models VCE-4200/4202/4210 vibrating wire strain gages*. Lebanon, NH: Author.

Larson, K.H., Peterman, R.J., & Esmaeily, A. (2007). *Evaluating the time-dependent deformation and bond characteristics of a self-consolidating concrete mix and the implications for pretensioned bridge applications* (Report No. FHWA-KS-07-1). Topeka, KS: Kansas Department of Transportation.

Precast/Prestressed Concrete Institute (PCI). (2004). *PCI design handbook* (6th ed.). Chicago, IL: Author.

RISA-2D (Version 5.5) [Computer software]. (2001). Foothill Ranch, CA: RISA Technologies, Inc.

Yang, Y., & Myers, J.J. (2005). Prestress loss measurements in Missouri's first fully instrumented high-performance concrete bridge. *Transportation Research Record, 1928*, 118–125.

Zokaie, T., Osterkamp, T.A., & Imbsen, R.A. (1991). *Distribution of wheel loads on highway bridges* (NCHRP Project 12-26 Final Report). Washington, DC: Transportation Research Board.

AD ASTRA PER ASPERA

Kansas

Department of Transportation